Multiple-scattering and DV-X_α theoretical determination of the local structure of SO_2/Pd(111)

2002 J. Phys.: Condens. Matter 14 3099

(http://iopscience.iop.org/0953-8984/14/12/303)

INSTITUTE OF PHYSICS PUBLISHING JOURNAL OF PHYSICS: CONDENSED MATTER

J. Phys.: Condens. Matter **14** (2002) 3099–3113 PII: S0953-8984(02)30645-3

Multiple-scattering and DV-X_α theoretical determination of the local structure of SO_2/Pd(111)

S Cao[1], **J-C Tang, L Wang, P Zhu and S L Shen**

Department of Physics, Zhejiang University, Hangzhou 310027, People's Republic of China

E-mail: caosong@css.zju.edu.cn and phytang@dial.zju.edu.cn

Received 8 November 2001, in final form 8 January 2002
Published 15 March 2002
Online at stacks.iop.org/JPhysCM/14/3099

Abstract

We have calculated the sulfur 1s near-edge x-ray absorption fine-structure (NEXAFS) spectra of SO_2 adsorbed on Pd(111) in terms of the multiple-scattering cluster and self-consistent field DV-X_α method. The physical origin of the resonances in the NEXAFS spectra has been unveiled. By the multiple-scattering calculation we have for the first time identified two weak features appearing in S K-shell NEXAFS of SO_2/Pd(111), which locate near the π^* and σ^* resonances respectively. Meanwhile, a self-consistent DV-X_α cluster calculation has been performed to confirm the above conclusion. Our calculation results for the local structure of SO_2/Pd(111) are broadly in agreement with those of Fourier-transform analysis of the surface-extended x-ray absorption fine structure.

1. Introduction

In recent years, surface chemistry of sulfur dioxide (SO_2), known to be the origin of the acid rain, has gained increasing interest because of its environmental importance [1–13]. It is well known that SO_2, as a ligand in transition-metal complexes, exhibits interesting properties with an unequalled diversity of bonding modes [14]. In the majority of cases it bonds either through its S only or through its S and at least one O atom. Compared with the rich knowledge of many aspects of coordination chemistry, only a little information is available on the corresponding SO_2–surface complexes. The few structural studies already display a comparable variety of bonding configurations for SO_2–surface complexes. To date, three different bond configurations have been elucidated through high-resolution electron energy loss spectroscopy (HREELS), normal-incidence x-ray standing wavefield (NIXSW), and surface-extended and near-edge x-ray absorption fine-structure (SEXAFS and NEXAFS) studies [2,5,8,11,13]. It is reported that SO_2 is adsorbed on Ag(110) with η^1 configuration with only the S atom interacting with the surface [2]; meanwhile, MSC theoretical investigation

[1] Author to whom any correspondence should be addressed.

of NEXAFS shows an η^2 configuration bonding via the S atom and one of the O atoms [11]. The NIXSW and NEXAFS study of SO_2/Ni(111) indicates that both the O and S atoms are implicated in bonding with the substrate with η^3 configuration [5,13]. Recently Terada *et al* [8] have performed SEXAFS and NEXAFS studies of SO_2/Pd(111), and concluded that SO_2 is adsorbed on Pd(111) with the molecular plane normal to the surface, via the S atom and one of the O atoms. This corresponds to the η^2 configuration, which is obviously different from that on Ni(111).

NEXAFS has been shown to be a *fingerprint* of the local structure near an absorbing atom [15], which contains much adsorption geometry information, but the information obtained directly from the NEXAFS data seems to be limited. To obtain enough information about an adsorption system from the experimental NEXAFS spectra, it is necessary to perform a theoretical analysis of the NEXAFS spectra. Two kinds of theoretical method could be employed to analyse the NEXAFS spectra. Firstly, we can utilize the dynamical theory of electron scattering in the surface region to analyse the NEXAFS process. The core-level electrons of a centre atom are excited by incident x-rays. The excited photoelectrons are scattered by atoms surrounding the centre and then transit into the unoccupied orbits or the shape resonance states of the centre atom, which complies with the conservation of the angular momentum. The multiple-scattering cluster (MSC) method is a powerful tool in studying NEXAFS processes. Our group has successfully employed the MSC method to analyse some adsorption systems [11–13,16], and obtained their adsorption information. On the other hand, we may analyse the NEXAFS spectra according to the electronic structure of the adsorption system. The NEXAFS process is related to the electron transition from the core level to the unoccupied antibonding states, especially the π^* and σ^* ones. Therefore, in principle we can calculate the excited electron states of the adsorption system by the self-consistent field (SCF) DV-X_α method, and obtain the unoccupied molecular orbitals associated with the resonances in NEXAFS. In principle, the two theoretical techniques mentioned above should be self-consistent. Recently Zhu *et al* [12] have employed the MSC and DV-X_α method to successfully study the decomposition of SO_2 on Cu(100) and clearly obtain the local structure of (SO + 2O)/Cu(100), which enlightens us to approach the NEXAFS of SO_2/Pd(111) and determines the local structure of the adsorbate–substrate system by the combination of two methods.

2. The MSC and DV-X_α theoretical method

NEXAFS and core-level photoelectron diffraction have the same physical origin; i.e., the core-level electrons of a centre atom are excited by incident x-rays. The excited photoelectrons are scattered by the atoms surrounding the excited one and then transit into the unoccupied antibonding states or leave the system. This property allows us to utilize the dynamic theory of photoelectron diffraction to calculate the wavefunction of an intermediate photoelectron in NEXAFS [16–20], then we can obtain the absorption cross section by the MSC method.

According to the multiple-scattering theory, the wavefunction of an intermediate photoelectron located at $\vec{R}$ can be written as [18]

$$\Phi(\vec{R}) = \int G(\vec{R},\vec{r})\left[-\frac{e}{mc}\vec{A}\cdot\vec{P}\right]\varphi_i(\vec{r})\,\mathrm{d}\vec{r} = GH_i|\varphi_i\rangle \tag{1}$$

where $\varphi_i(\vec{r})$ is the initial wavefunction of the electron. $\vec{A}$ and $\vec{P}$ denote the x-ray vector potentials and electron momentum operators, respectively. G can formally be expressed in terms of $G_\circ$ and T,

$$G = G_\circ + G_\circ T G_\circ \tag{2}$$

where $G_\circ$ is the free-electron propagator and T is the T-matrix of the entire system. We may extract the single-atom scattering vertex t_α from T and call all remaining scattering events T',

$$G = (1 + G_\circ T')(G_\circ + G_\circ t_\alpha G_\circ); \tag{3}$$

in equation (3), the remaining scattering matrix T' is defined as

$$T' = \sum_{\beta\neq\alpha} t_\beta + \sum_{\gamma\neq\beta}\sum_{\beta\neq\alpha} t_\gamma G_\circ t_\beta + \cdots \tag{4}$$

in which $\alpha, \beta, \gamma, \ldots$ are the atoms in the cluster considered, and α represents the central atom (absorption centre). Obviously, $\Phi(\vec{R})$ can be separated into two parts,

$$\Phi(\vec{R}) = \Phi_D(\vec{R}) + \Phi_S(\vec{R}) \tag{5}$$

$$\Phi_D(\vec{R}) = (G_\circ + G_\circ t_\alpha G_\circ) H_i |\varphi_i\rangle \tag{6}$$

where $\Phi_D(\vec{R})$ represents direct emission of the photoelectron from the central atom and $\Phi_S(\vec{R})$ the scattering wavefunction. It can be shown that the asymptotic form of $\Phi_D(\vec{R})$ is

$$\Phi_D(\vec{R}) \sim \frac{2m}{\hbar^2}\frac{\mathrm{e}^{\mathrm{i}kR}}{R}\mathrm{e}^{-\mathrm{i}\vec{k}\cdot\vec{R}_\alpha}\sum_L Y_L(\vec{R})M_L^\alpha = \frac{\mathrm{e}^{\mathrm{i}kR}}{R}\Phi_\circ(k,\vec{R}), \qquad \vec{R}\to\infty \tag{7}$$

in which $\Phi_\circ(k,\vec{R})$ is the amplitude of the direct emission, and the excitation matrix element M_L^α is written as

$$M_L^\alpha = -(-\mathrm{i})^L \int \mathrm{e}^{\mathrm{i}\delta_L^\alpha}\xi_L^\alpha(\rho)Y_L^*(\vec{\rho})\left[-\frac{e}{mc}\vec{A}\cdot\vec{P}\right]\varphi_i(\vec{\rho})\,\mathrm{d}\vec{\rho} \tag{8}$$

where L is the (l, m) pair, δ_L^α is the lth phase shift and $\xi_L^\alpha(\rho)Y_L^*(\vec{\rho})$ is the excited state of the centre atom α, which we calculate by the SCF-X_α method. It is important to point out that l is controlled by the selection rule of angular momentum. For K-edge NEXAFS, the $\varphi_i(\vec{r})$ is the s state, $l_i = 0$, so for the final angular momentum $l = 1$, i.e. the p state. From the above equations, we can find that the scattering wave is an infinite series [17, 20],

$$\Phi_S(\vec{R}) = \sum_{n=1}^{\infty}\Psi_n(\vec{R}) \tag{9}$$

in which the first term is given by

$$\begin{aligned}\Psi_1(\vec{R}) &= \sum_{\beta\neq\alpha} G_\circ t_\beta \Phi_D \sim \frac{2m}{\hbar^2}\frac{\mathrm{e}^{\mathrm{i}kR}}{R}\sum_{\beta\neq\alpha}\mathrm{e}^{-\mathrm{i}\vec{k}\cdot\vec{R}_\beta}\sum_{LL'}Y_{L'}^*(\vec{R})t_{l'}^\beta G_{L'L}(\vec{R}_\beta - \vec{R}_\alpha)M_{LL'}^\alpha \\ &= \frac{\mathrm{e}^{\mathrm{i}kR}}{R}\Phi_1(k,\vec{R}), \qquad R\to\infty.\end{aligned} \tag{10}$$

We define a matrix $Q(\alpha,\beta)$ in the following way:

$$Q(\alpha,\beta) = \begin{cases} 0 & \beta = \alpha \\ t_{l'}^\beta G_{L'L}(\vec{R}_\beta - \vec{R}_\alpha) & \beta\neq\alpha \end{cases} \tag{11}$$

then the amplitude of the first scattering term can be written as

$$\Phi_1(k,\vec{R}) = \sum_{\beta\neq\alpha} G_\circ t_\beta \Phi_D \sim \frac{2m}{\hbar^2}\sum_{\beta\neq\alpha}\mathrm{e}^{-\mathrm{i}\vec{k}\cdot\vec{R}_\beta}\sum_{LL'}Y_{L'}^*(\vec{R})Q_{\beta L'}^{\alpha L}M_{LL'}^\alpha. \tag{12}$$

For the double-scattering term, we have

$$\begin{aligned}\Psi_2(\vec{R}) &= \frac{\mathrm{e}^{\mathrm{i}kR}}{R}\Phi_2(k,\vec{R}) \\ \Phi_2(k,\vec{R}) &= \frac{2m}{\hbar^2}\sum_{\gamma\neq\beta}\sum_{\beta\neq\alpha}\mathrm{e}^{-\mathrm{i}\vec{k}\cdot\vec{R}_\gamma}\sum_{LL'L''}Y_{L''}^*(\vec{R})Q_{\gamma L''}^{\beta L'}Q_{\beta L'}^{\alpha L}M_{LL'}^\alpha, \qquad R\to\infty.\end{aligned} \tag{13}$$

In the same manner, the asymptotic expression of the scattering wave can be summarized by the $\hat{Q}$ matrix and the excitation matrix:

$$\Phi_S(\vec{R}) = \frac{e^{ikR}}{R}\sum_n \Phi_n(k,\vec{R})$$
$$\sum_n \Phi_n(k,\vec{R}) = \frac{2m}{\hbar^2}\sum_\gamma e^{-i\vec{k}\cdot\vec{R}_\gamma}\sum_{L_1} Y^*_{L_1}(\vec{R})\left[\frac{\hat{Q}}{1-\hat{Q}}\right]^{\gamma L_1}_{\alpha L} M^\alpha_{LL'}, \qquad \vec{R}\to\infty \tag{14}$$

where γ represents the scattering atom. The multiple-scattering process of the excited photoelectrons in NEXAFS shows strong localization because of their low energy, so we can choose an adsorbed molecule and a few neighbouring atoms (about 30) in the substrate to construct a cluster which simulates the adsorption system. In the MSC method, it is assumed that the absorption cross section of x-rays is proportional to the emission cross section of the intermediate photoelectrons; in such a way, we find the total cross section σ,

$$\sigma = c\int\left|\Phi_\circ + \sum_{n=1}^{\infty}\Phi_n\right|^2 d\Omega \tag{15}$$

where c is a proportional constant. The modulation function is defined as

$$\chi(k) = \frac{\sigma-\sigma_0}{\sigma_0} \tag{16}$$

$$\sigma_0 = c\int|\Phi_\circ|^2\, d\Omega, \tag{17}$$

σ_0 is the absorption background and $\chi(k)$ can then be compared with experimental spectra.

To reveal the properties of the lower unoccupied molecular orbitals (LUMOs) of the cluster associated with the resonances in NEXAFS and compare them with the above MSC calculation, we perform a DV-X_α calculation for the same system. The DV-X_α cluster method [21,22] is one of the most useful techniques for solving the Harttree–Fock–Slater (HFS) equation based on statistical approximation to the exchange–correlation potential. The method provides accurate electronic structures for complex systems in less computer time [23]. Recently, two of the present authors have made a DV-X_α calculation that connects the LUMO of (SO + 2O) + 6Cu cluster with the individual resonances in the NEXAFS spectra of the SO_2/Cu(100) system at room temperature [12]. By means of the DV-X_α method, we can calculate the cluster wavefunction and the corresponding molecular orbitals, which are useful to analyse the transition probability and identify the resonances in NEXAFS spectra.

3. Results and discussion

3.1. The features of experimental NEXAFS and the orientation of the SO_2 molecule

The S K-shell NEXAFS spectra of SO_2/Pd(111) measured by Terada *et al* [8] are plotted in figure 1(*a*). There are two precise peaks assigned correctly as π^* and σ^* resonances appearing in the experimental spectra, which are similar to those of multilayer SO_2 [8], but there is no assignment to the broad structure in figure 1(*a*), which we labelled as resonance ***A***. By a direct inspection, one can find that there exists a weak feature labelled as ***X*** about 10 eV above the π^* resonance at grazing incidence ($\theta = 1^\circ$), whose physical origin has never been discussed before. Furthermore, we noticed that the π^* resonance is complicated, i.e. the peak position locates at 2474 eV at normal incidence while at grazing incidence ($\theta = 1^\circ$) it shifts towards lower energy by about 1 eV even though its intensity is rather weaker. We label this weak

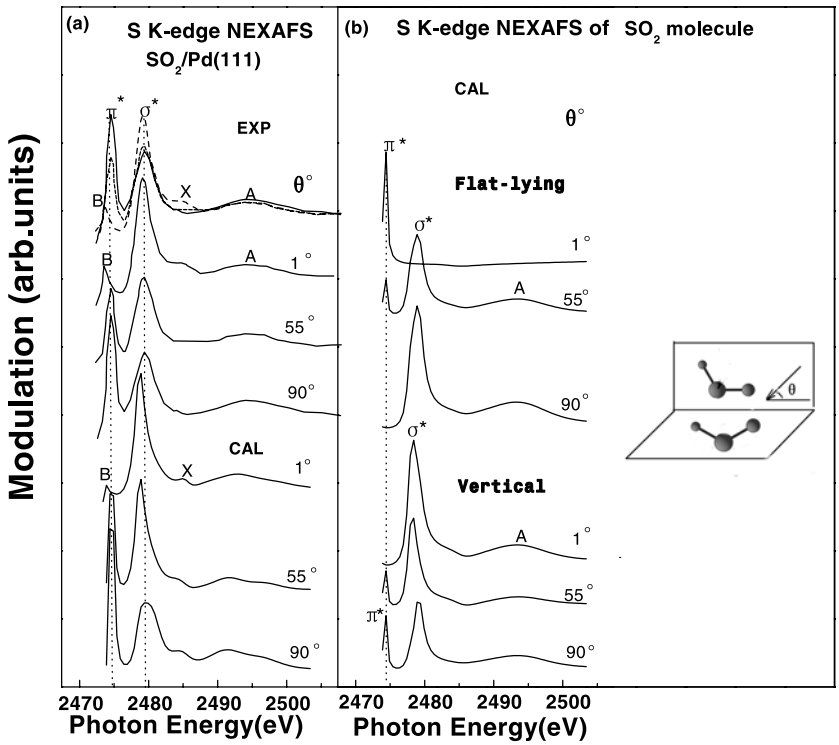

Figure 1. (*a*) The experimental and calculated S 1s NEXAFS spectra of SO_2/Pd(111). (*b*) The calculated S 1s NEXAFS spectra of two orientations of SO_2 molecule at three incident angles. The experimental spectra are quoted from [8].

resonance as peak $\boldsymbol{B}$. This leads to the following question: what is the origin of peak $\boldsymbol{B}$? Meanwhile, we observed that the π^* and σ^* peaks exhibit opposite polarization dependence to each other; the π^* peak is enhanced at normal x-ray incidence, while the σ^* peak reaches its maximum at grazing incidence ($\theta = 1^\circ$).

In order to investigate the orientation of the SO_2 molecule in SO_2/Pd(111) and achieve a better understanding of the experimental spectra, we have performed an MSC calculation of S 1s NEXAFS for two orientations of the SO_2 molecule, i.e. the flat-lying one and the vertical one shown in figure 1(*b*). In our calculation, the calculated structural parameters are as follows: the S–O intramolecular bond length is taken as 1.43 Å, a commonly accepted bond length value for gas-phase sulfur dioxide, and the OSO bond angle as 120°. Because there are three equivalent azimuths for SO_2 adsorbed on Pd(111), we have to take the average over them in the above calculation. It is shown in figure 1(*b*) that the π^* resonance is strongly excited for the flat-lying one at grazing incidence ($\theta = 1^\circ$), otherwise for the vertical one. Based on the π^* intensity of the experimental spectrum, which is very weak to be excited at $\theta = 1^\circ$, it is reasonable to conclude that the molecular plane of SO_2 on Pd(111) should be normal to the surface.

The S K-shell NEXAFS spectrum of gas-phase sulfur dioxide has been measured by Bodeur and Esteva [24]. They pointed out that the first and the second peaks were assigned to the π^* and σ^* resonances, but they did not assign the broad structure which we labelled as resonance $\boldsymbol{A}$. In order to illustrate the properties of these resonances, we carry out a DV-X_α calculation. In the calculation, the structural parameters are taken to be the same as those of

Table 1. Energy levels (eV) and orbital configuration of LUMO of SO_2 by DV-X_α calculation.

Symbol	Energy (eV)	The major configuration of the orbital	Assigned peaks
H	0.0	**S(3p)0.1223**, S(3d)0.1277, O(2p)0.6514	(HOMO)
b_1	3.76	**S(3p)0.49**, S(3d)0.08, O(2p)0.43	π^*
a_1	9.06	S(3s)0.09, **S(3p)0.28**, S(3d)0.39, O(2s)0.01, O(2p)0.23	σ^*
b_2	9.82	**S(3p)0.38**, S(3d)0.38, O(2s)0.01, O(2p)0.22	
A_1	24.22	S(3s)0.08, **S(3p)0.05**, S(3d)0.65, O(2s)0.06, O(2p)0.16	***A***
A_2	30.24	**S(3p)0.26**, S(3d)0.51, O(2s)0.08, O(2p)0.16	

gas-phase sulfur dioxide, which have been shown in the above MSC calculation. The energy levels of the LUMO of the gas-phase SO_2, which is relative to the highest occupied molecular orbital (HOMO), are listed in table 1, while the corresponding contour maps are given in figure 2. *Meanwhile, we identify the positions of the atoms of the SO_2 molecule in certain panels which can apply to all panels in figure 2.* In addition, we find there are two levels (24.22 and 30.24 eV) corresponding to the resonance ***A*** and their energy interval is equal to 6.02 eV, so far as this weak feature is a very broad one as seen in figure 1. In figure 2 we omit one orbit map of the ***A*** resonance because its S(3p) component is too small (see table 1). These contour maps are plotted on two planes, i.e. the left-hand one is parallel to the molecule plane and the right-hand one is perpendicular to the former. Their plots are denoted by x-1 and x-2, respectively. Figure 2 shows that the lowest unoccupied orbital of SO_2 is antisymmetric to the S–O bond, which means the orbital is an antibonding π^* orbital. The next two unoccupied orbitals exhibit a approximate global symmetry around the S–O bond. Obviously they correspond to the σ^* orbitals. According to the group theory, the C_{2v} symmetry of the SO_2 molecule implies that the antibonding orbital π^* corresponds to the b_1 irreducible representation while the σ^* orbital contains two nearby antibonding states a_1 and b_2, which was suggested in [24]. By an inspection of figure 2, we find that the ***A*** resonance is a σ^*-like one, which displays approximate global symmetry around the S–O bond.

3.2. Optimized structure model of SO_2*/Pd(111)*

Based on the S k-edge NEXAFS experiment of SO_2/Pd(111) performed by Terada *et al* [8], we draw the schematic diagram of the system in figure 3(a), where the S atom takes a bridge site and one oxygen atom is close to the bridge site. In our calculation, we have optimized all geometry parameters in the model, and plotted the result in figure 1(a) to compare with the experimental spectra. In the calculation, the adsorption height h (the distance between the S atom and the first layer of the substrate) is taken as 1.7 Å, and the molecular plane is normal to the surface and the C_2 axis tilted by 20° from the surface normal. The two different intramolecular S–O bond lengths are set at 1.40 Å for the upright one and 1.48 Å for the almost surface-parallel one, and the OSO bond angle α is taken as 120°. The incident angle (θ) of the x-rays with respect to the surface changes from 1° to 90°. Because there are three equivalent azimuths for the SO_2 adsorbed on Pd(111), we have to take the average over them. Obviously figure 1(a) shows that the calculated spectra are in good agreement with the experimental data. Our MSC calculation supports the experimental result suggested by Terada *et al* [8]. Their SEXAFS analyses indicate that the S atom is adsorbed on the bridge site of Pd(111), while inequivalent intramolecular S–O bonds are identified with the distances of 1.43 Å for the upright one and 1.48 Å for the surface-parallel one. It is interesting that the calculated

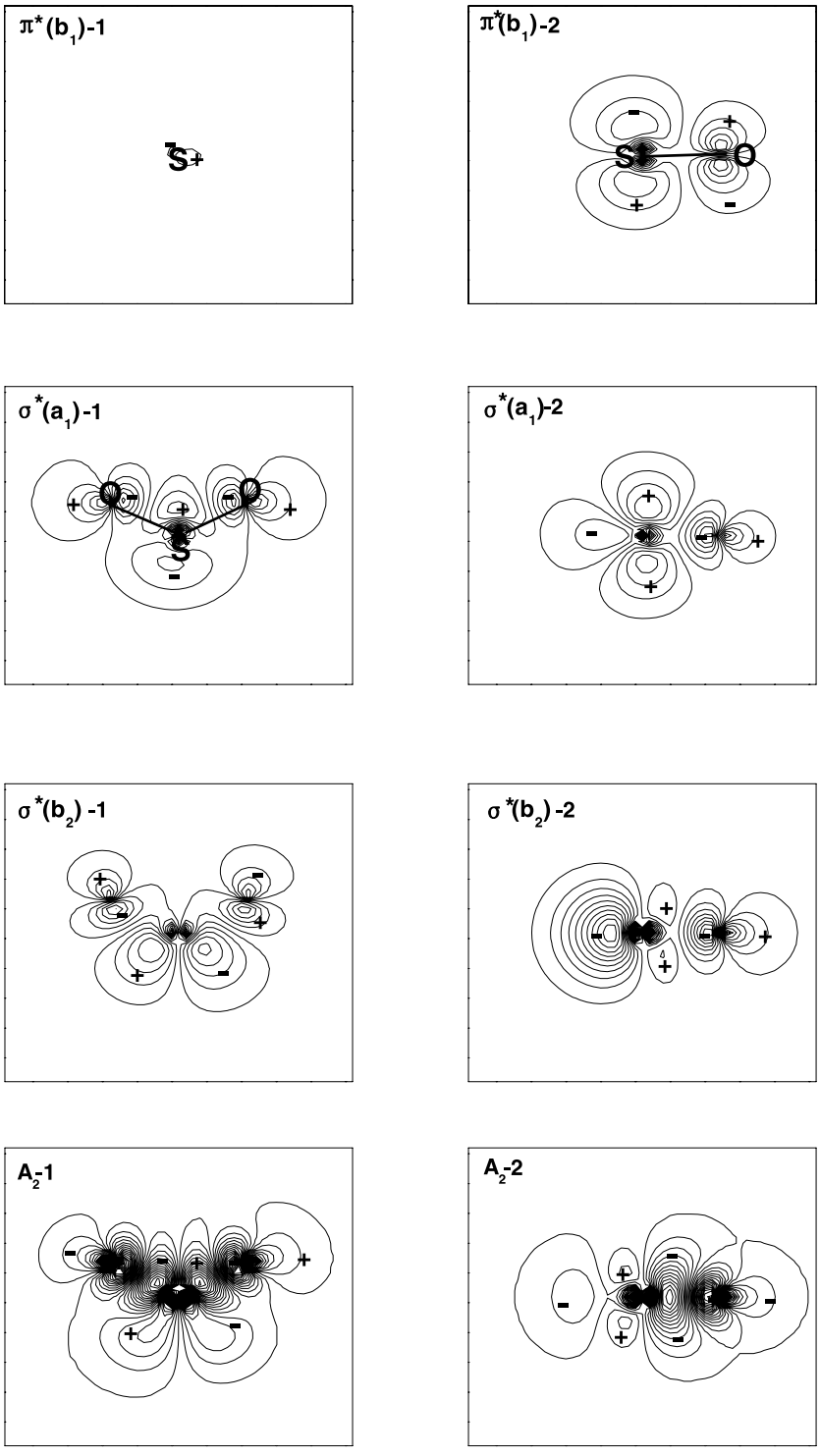

Figure 2. Contour maps of the four lowest unoccupied orbitals of SO_2 due to DV-X_α studies, which correspond to the peaks in NEXAFS.

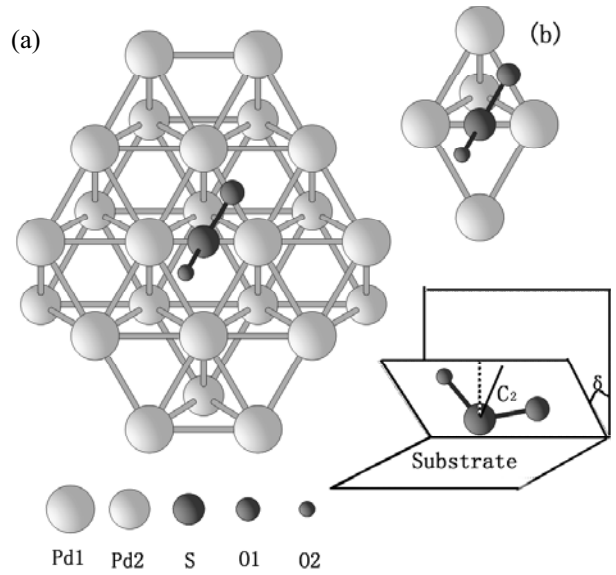

Figure 3. Schematics of the adsorption structure SO_2/Pd(111). (*a*) MSC calculation clusters; (*b*) DV-X_α calculation cluster.

S 1s NEXAFS spectrum of the SO_2 molecule is similar to that of SO_2/Pd(111) except the π^* and $\boldsymbol{X}$, which we shall study in detail lately. This fact shows that the main contribution to the NEXAFS spectra of the adsorption system SO_2/Pd(111) is due to the adsorbate.

3.3. The physical origin of two weak structures

3.3.1. Peak $\boldsymbol{X}$. Now we inspect the weak feature in figure 1. Both the calculated spectrum and the experimental one exhibit a weak feature $\boldsymbol{X}$ at grazing incidence ($\theta = 1^\circ$). In order to understand the physical cause of peak $\boldsymbol{X}$, we calculated the NEXAFS spectra at different adsorption heights while keeping other parameters the same as in figure 1(*a*). Figure 4 shows the comparison between the calculated spectra of different adsorption heights and the experimental one at grazing incidence. It is observed that peak $\boldsymbol{X}$ moves to lower energy as h increases; this property shows that weak resonance $\boldsymbol{X}$ is closely correlated with the adsorption height of the SO_2 molecule. The strong dependence of peak $\boldsymbol{X}$ on the adsorption height indicates that the peak is attributable to the interaction between the SO_2 molecule and the substrate. Later a DV-X_α cluster calculation will prove this judgement.

Peak $\boldsymbol{X}$ is closely related to the interaction between the substrate and adsorbate, so we can determine the adsorption height according to its intensity and position. It is observed in figure 4 that the calculated curve, corresponding to $h = 1.7$ Å, is in agreement with experiment because the position and intensity of the $\boldsymbol{X}$ peak fit the experimental one as well. Therefore, we conclude that $h = 1.7 \pm 0.1$ Å, from which we can deduce $L_{\mathrm{S-Pd}}$ (the bond distance between S and Pd) equal to 2.2 ± 0.1 Å. The S–Pd bond length agrees fairly well with the experimental result [8]. Meanwhile, we obtain the distance between the almost surface-parallel O atom (O1) and the Pd atom, which is equal to 2.4 ± 0.1 Å. These confirm the η^2 configuration of SO_2/Pd(111), in which the S atom and one of the O atoms directly bond and interact with the Pd atoms in the substrate.

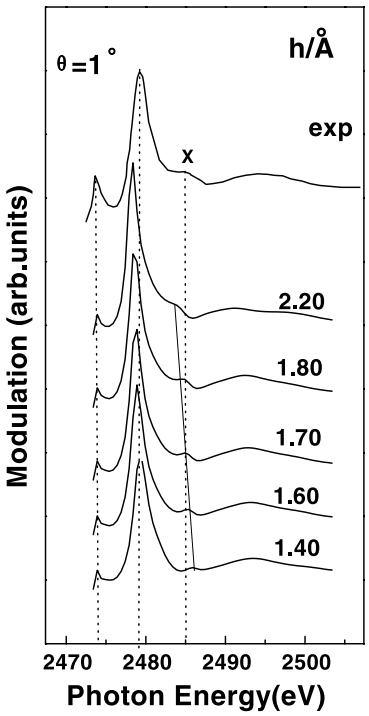

Figure 4. Comparison between the experimental spectrum and the calculated S 1s NEXAFS spectra corresponding to different adsorption heights (h) at grazing incidence ($\theta = 1^\circ$). The adsorption height changes from 1.40 to 2.20 Å.

3.3.2. Peak $\boldsymbol{B}$. We have noticed that the position of peak $\boldsymbol{B}$ at grazing incidence ($\theta = 1^\circ$) is different from the π^* position at the incidence angle $\theta = 55^\circ$ by about 1 eV. To gather more information about the $\boldsymbol{B}$ peak, we plot the calculated spectra with different molecular plane tilt angle (δ) in figure 5 with other parameters taken to be the same as in figure 1(a). When δ changes from 0° to 30°, we can see that the $\boldsymbol{B}$ and π^* peaks appear alternately, i.e. when $\delta = 10^\circ$, peak $\boldsymbol{B}$ is coincident with π^* while as $\delta = 0^\circ$ it deviates from π^* by about 1 eV. Therefore, we can conclude that peak $\boldsymbol{B}$, which originates from the interaction between the adsorbate and the substrate, is a new resonance. Our SCF DV-X_α analysis will further confirm the above judgement.

Angle-dependent NEXAFS analysis gave a value of less than 10° for the orientation angle (δ) of the molecular plane from the surface normal [8]. We can determine the orientation angle according to figure 5 mentioned above. It is not difficult to find that the calculated curve, corresponding to $\delta = 0^\circ$, is in fairly good agreement with the experimental spectrum because both the position and intensity of peak $\boldsymbol{B}$ fit the experimental one as well. Therefore, we judge that the molecular plane is normal to the surface in the SO_2/Pd(111) adsorption system, which confirms the angle-dependent NEXAFS analysis result.

3.4. Determination of the two S–O bond lengths

Due to the inequivalence of the two oxygen atoms of the SO_2/Pd(111) adsorption system, two different intramolecular S–O bond lengths have been identified by the SEXAFS experiment [8]. To demonstrate the result, we have calculated individually the NEXAFS spectra with different

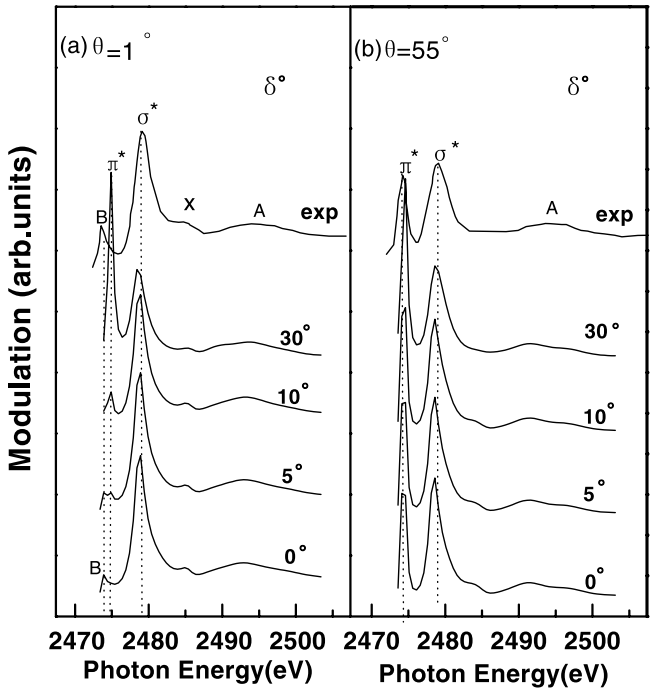

Figure 5. Plot of the calculated S 1s NEXAFS spectra of SO_2/Pd(111) versus the molecular plane tilt angle (δ) at two grazing incidences ($\theta = 1^\circ$ and 55°). δ changes from 0° to 30°.

S–O intramolecular bond lengths of the upright one (Ls-o2) and the surface-parallel one (Ls-o1). The MSC calculation shows that the intensity ratio of π^* to σ^* is sensitive to the S–O bond lengths, which makes it possible to determine the S–O intramelocular bond lengths. Figure 6(*a*) exhibits the comparison between the relative intensities of the calculated π^*/σ^* and those in the experiment, where Ls-o1 is varied but the other parameters in the calculation are kept at the same values as in figure 1(*a*). Obviously, the calculated curve, corresponding to Ls-o1 = 1.48 Å, shows the best fit to the experimental one. Therefore, we judge that Ls-o1 is equal to 1.48 ± 0.03 Å. Similarly figure 6(*b*) shows the comparison between that corresponding to Ls-o2 and those in the experimental one, while the other parameters in the calculation are kept the same as in figure 1(*a*). A similar judgement as above gives the conclusion that Ls-o2 is equal to 1.40 ± 0.03 Å. Our conclusion supports the SEXAFS experimental result on the inequivalent intramolecular S–O bonds [8]. Two different intramolecular S–O bond lengths appearing in the same molecule were also indicated in the SO_2/Cu(111) adsorption system [6]. The additional bonding of the surface-parallel oxygen atom with the substrate can explain the surface-parallel S–O bond elongation.

3.5. SCF DV-X_α analysis

To reveal the properties of the LUMO of the cluster associated with the resonances in NEXAFS and compare them with the above MSC calculation, we perform a DV-X_α calculation for both the SO_2 molecule and SO_2/Pd(111) adsorption system.

Our MSC calculation revealed that two weak structures appear in S K-edge NEXAFS after SO_2 is adsorbed on the Pd(111) surface. To confirm the above result, we carry out a DV-X_α

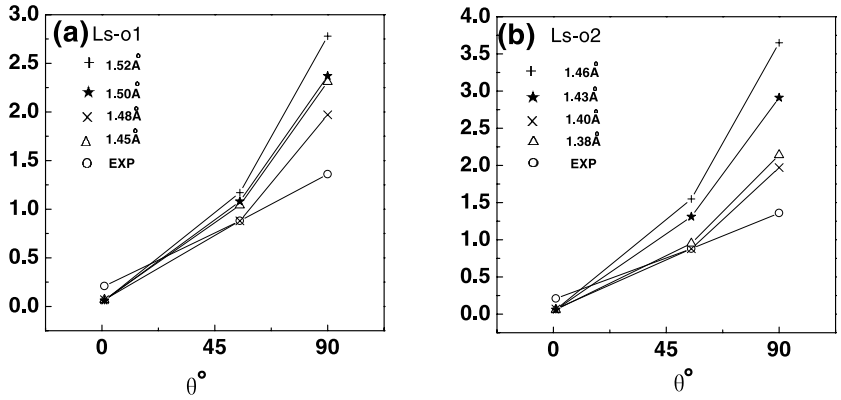

Figure 6. Comparison between the experimental intensity ratio of π^*/σ^* and those of the MSC calculation for the same ones. (*a*) Bondlength Ls-o1 changes from 1.45 to 1.52 Å. (*b*) Bondlength Ls-o2 changes from 1.38 to 1.46 Å. The circles (○) represent the experimental data in both panels.

calculation for the SO_2 + 5Pd cluster which simulates the adsorption system SO_2/Pd(111) shown in figure 3(*a*), and all the parameters are same as those for the MSC study. Nine LUMO energy levels of the SO_2+5Pd cluster, which contain a comparable amount of S(3p) component, are listed in table 2. Making a careful comparison between the energy levels listed in tables 1 and 2 it is no difficulty to find that the levels marked b_1, a_1, b_2, A_1,and A_2 in table 2 are one by one corresponding to all LUMO levels in table 1. Thereafter, we plot the contour maps of these partners of table 1 in two planes (see figure 7), in which the left-hand panel (labelled by x-1) is parallel to the adsorbate plane and the right-hand one (labelled by x-2) is perpendicular to the former and through the S–O1 axis. By a direct inspection of figure 7, we can find that all contour maps plotted in the x-2 plane are similar to the corresponding orbitals in figure 2 because the lateral interaction between the adsorbate and the substrate is rather weaker. The remaining levels in table 2 lack partners in table 1. Fortunately, these two sets of LUMO levels correspond to the weak features $\boldsymbol{B}$ and $\boldsymbol{X}$ identified by the above MSC calculation. Obviously the set (B_1, B_2) near π^* shows the character of the weak peak $\boldsymbol{B}$, while the set (X_1, X_2) about 10 eV above π^* acts the role of peak $\boldsymbol{X}$. Their contour maps, found in the SO_2+5Pd cluster, are plotted in figure 8. The two planes (x-1, x-2) for every orbital are defined as follows. The x-1 plane is parallel to the S–Pd bonding plane and the x-2 plane is similarly defined as in figure 7. It is easy to find that the two new weak structures are very complicated in the x-1 planes and display the π^* and σ^* orbital properties in the x-2 planes respectively, which originate from the interaction between the adsorbate and the substrate suggested by MSC calculation.

4. Conclusions

We have investigated the S K-shell NEXAFS spectra of gas-phase SO_2 and SO_2 adsorbed on the Pd(111) surface by both the MSC and DV-X_α methods. The MSC calculation shows for the first time that there exist two weak features, which locate near and 10 eV higher than π^* respectively, in the SO_2/Pd(111) adsorption system. This is confirmed by DV-X_α calculation. We obtain the local structure of the SO_2/Pd(111) adsorption system, which is similar to the conclusion suggested by SEXAFS analysis. The new η^2 configuration of SO_2/Pd(111) is confirmed by MSC calculation.

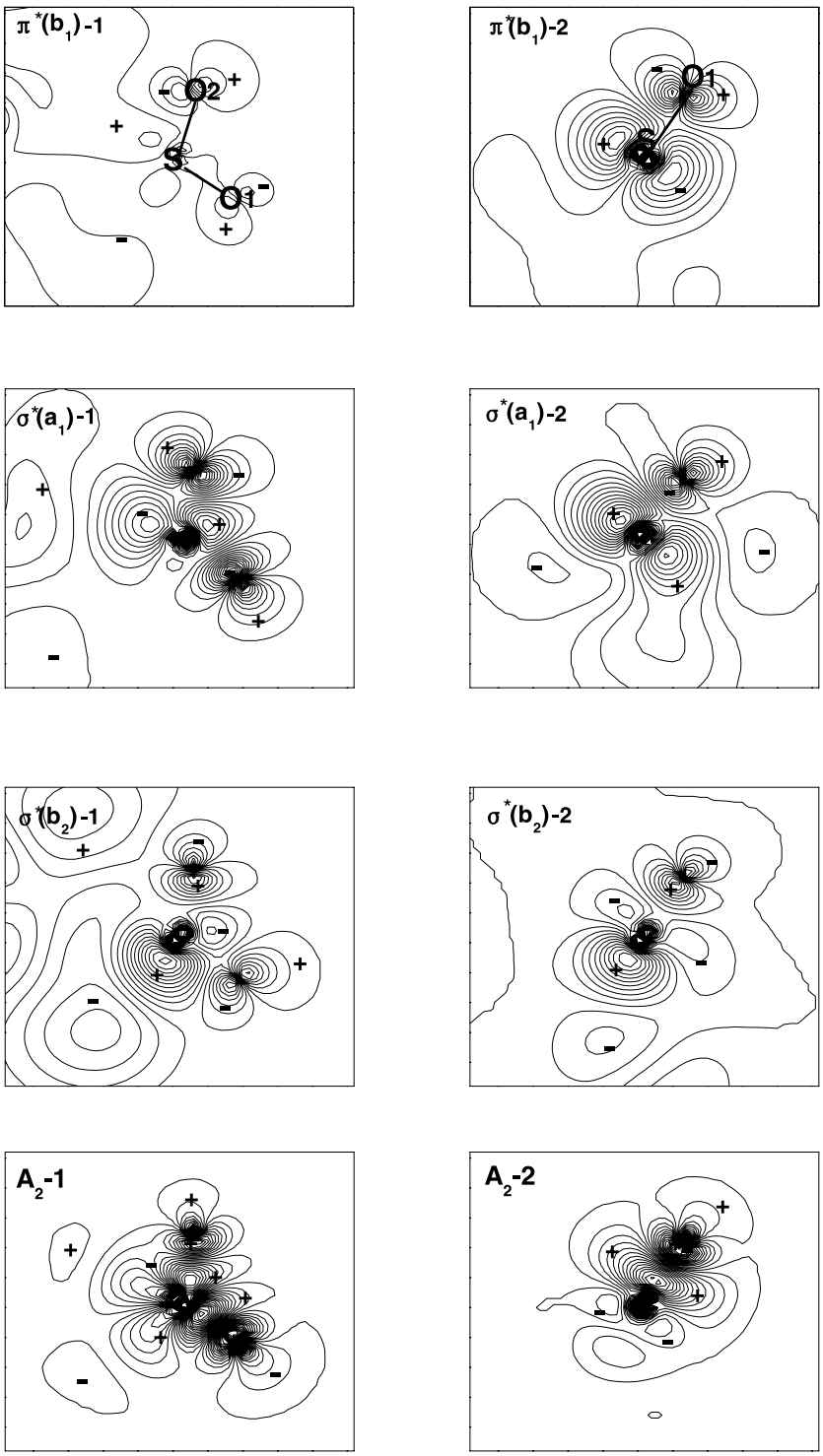

Figure 7. Contour maps of LUMO of SO_2/Pd(111) corresponding to those plotted in figure 2.

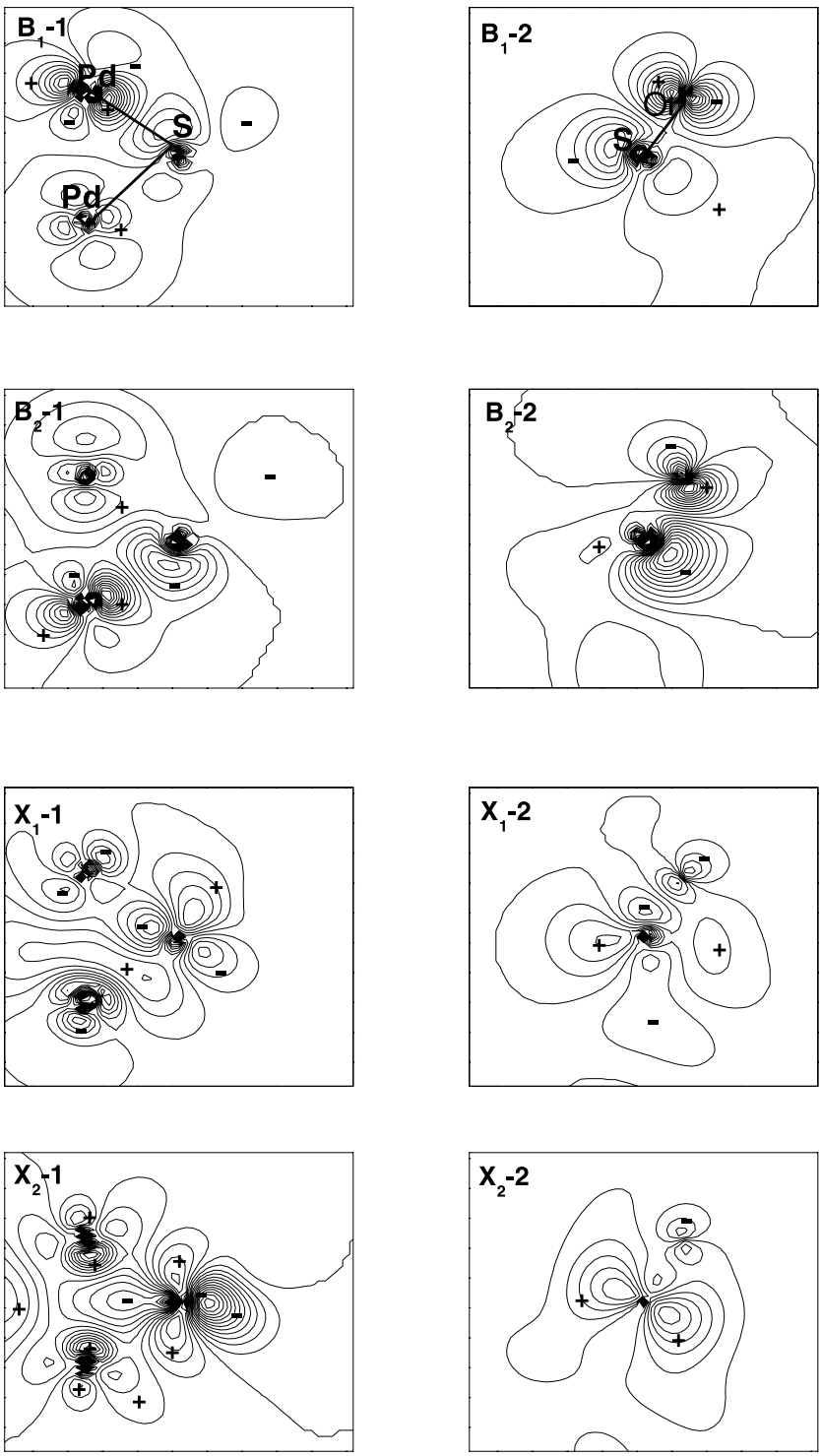

Figure 8. Contour maps of the orbitals associated with the weak peaks in NEXAFS of SO_2/Pd(111).

Table 2. Energy levels (eV) and orbital configuration of the LUMO of the SO_2 + 5Pd cluster by DV-X_α calculation.

Symbol	Energy (eV)	The major configuration of the orbital	Assigned peaks
H	0.0	Pd1(4d)0.64, Pd1(5s)0.11, Pd1(5p)0.10, Pd2(5s)0.06	(HOMO)
B_1	0.50	**S(3p)0.08**, O1(2p)0.08, O2(2p)0.06, Pd1(4d)0.37, Pd1(5s)0.16, Pd1(5p)0.12, Pd2(4d)0.08	$\boldsymbol{B}$
B_2	0.80	**S(3p)0.07**, O1(2p)0.05, O2(2p)0.05, Pd1(4d)0.17, Pd1(5s)0.39, Pd1(5p)0.13	
b_1	1.71	**S(3p)0.13**, O1(2p)0.03, O2(2p)0.05, Pd1(5s)0.26, Pd1(5p)0.28, Pd1(5p)0.13	π^*
a_1	6.87	S(3s)0.06, **S(3p)0.15**, S(3d)0.17, O1(2p)0.08, O2(2p)0.08, Pd1(5p)0.23, Pd2(5p)0.15	σ^*
b_2	8.01	**S(3p)0.12**, S(3d)0.05, O1(2p)0.02, O2(2p)0.02, Pd1(4d)0.06, Pd1(5p)0.55, Pd2(5p)0.16	
X_1	13.23	**S(3p)0.01**, S(3d)0.25, O1(2p)0.01, O2(2p)0.03, Pd1(5s)0.06, Pd1(5p)0.42, Pd2(5p)0.12	$\boldsymbol{X}$
X_2	13.49	**S(3p)0.04**, S(3d)0.50, O1(2p)0.05, O2(2p)0.04, Pd1(5p)0.18, Pd2(5p)0.09	
A_1	22.79	**S(3p)0.08**, S(3d)0.62, O1(2s)0.04, O1(2p)0.09, O2(2p)0.04, Pd1(5p)0.06	$\boldsymbol{A}$
A_2	28.45	**S(3p)0.18**, S(3d)0.53, O1(2p)0.04, O2(2p)0.12	

(a) The main contribution to the S 1s NEXAFS spectra of SO_2/Pd(111) is derived from the SO_2 molecule. The molecular plane of SO_2 is normal to the surface.
(b) Two new features, labelled as $\boldsymbol{B}$ and $\boldsymbol{X}$, are indicated by both the experimental NEXAFS spectra and MSC calculation, which originate from the interaction between SO_2 and the substrate Pd(111); especially the X resonances are due to the interaction between S(3d) and Pd(5p).
(c) In SO_2/Pd(111), the SO_2 molecule is adsorbed in the bridge site with only one O atom and the S atom implicated in bonding, which corresponds to the η^2 configuration. The adsorption height of SO_2 is 1.7 ± 0.1 Å.
(d) Compared with gas phase SO_2, inequivalent intramolecular S–O bonds are clearly identified with the distances of 1.40 ± 0.03 Å for the upright one and 1.48 ± 0.03 Å for the surface-parallel one. The elongation of the surface-parallel S–O bond is derived from the additional bonding between the oxygen and the substrate.

Acknowledgments

The authors acknowledge the support of the National Natural Science Foundation of China, grant no 19974036. The authors are grateful to Dr B Song for the useful discussion about DV-X_α calculations. Most of the numeric calculations involved in this research were performed on the super-computing server of the Centre of Numeric Simulation and Scientific Computing, Zhejiang University.

References

[1] Yokoyama T, Terada S, Yagi S, Imanishi A, Takenaka S, Kitajima Y and Ohta T 1995 *Surf. Sci.* **324** 25
[2] Guitiérrez-Sosa A, Walsh J F, Muryn C A, Finetti P, Thornton G, Robinson A W, Addato S D' and Frigo S P 1996 *Surf. Sci. Lett.* **364** L519
[3] Pangher N, Wilde L, Polcik M and Haase J 1997 *Surf. Sci.* **372** 211
[4] Nakahashi T, Terada S, Yokoyama T, Hamamatsu H, Kitajima Y, Sakano M, Matsui F and Ohta T 1997 *Surf. Sci.* **373** 1

[5] Jackson G J, Lüdecke J, Driver S M, Woodruff D P, Jones R G and Chan A 1997 *Surf. Sci.* **389** 223
[6] Polčik M, Wilde L and Haase J 1998 *Phys. Rev.* B **57** 1868
[7] Wilde L, Polčik M, Haase J, Brena B, Cocco D, Comelli G and Paolucci G 1998 *Surf. Sci.* **405** 215
[8] Terada S, Yokoyama T, Sakano M, Kiguchi M, Kitajima Y and Ohta T 1999 *Chem. Phys. Lett.* **300** 645
[9] Terada S, Yokoyama T, Okamoto Y, Kiguchi M, Kitajima Y and Ohta T 1999 *Surf. Sci.* **442** 141
[10] Jackson G J, Driver S M, Woodruff D P, Abrams N, Jones R G, Butterfield M T, Crapper M D, Cowie B C C and Formoso V 2000 *Surf. Sci.* **459** 231
[11] Zhu P, Tang J C and He J P 2000 *Phys. Chem. Chem. Phys.* **2** 1123
[12] Zhu P, Tang J C and He J P 2000 *J. Phys. Chem.* B **104** 10 597
[13] Cao S, Tang J-C, Zhu P and Wang L 2001 *J. Phys.: Condens. Matter* **13** 5865
[14] Ryan B R, Kubas G J, Moody D C and Eller P G 1981 *Struct. Bonding* **46** 47
[15] Stöhr J 1992 *NEXAFS Spectroscopy (Springer Series in Surface Science 25)* ed R Gomer (Berlin: Springer)
[16] Tang J C, Feng X S, Shen J F, Fujikawa T and Okazawa T 1991 *Phys. Rev.* B **44** 13 018
[17] Tang J-C, Fu S-B, Ji H and Chen Y-B 1992 *Sci. China* A **35** 965
[18] Liebsch A 1976 *Phys. Rev.* B **13** 544
[19] Fujikawa T 1981 *J. Phys. Soc. Japan* **50** 1321
[20] Fujikawa T 1981 *J. Electron. Spectrosc. Relat. Phenom.* **22** 353
[21] Averill F W and Ellis D E 1973 *J. Chem. Phys.* **59** 6412
[22] Adachi H, Tsukada M and Satoko C 1978 *J. Phys. Soc. Japan* **45** 875
[23] Song B, Nakamatsu H, Sekine R, Mukoyama T and Taniguchi K 1998 *J. Phys.: Condens. Matter* **10** 9443
[24] Bodeur S and Esteva J M 1985 *Chem. Phys.* **100** 415